Gliding discharge plasma-catalytic system for decomposition of ammonia as a chemical carrier of hydrogen

Michał Młotek* [ID] , Maria Ogrodowska, Michalina Perron [ID] , Bogdan Ulejczyk [ID] , Krzysztof Krawczyk [ID]

Warsaw University of Technology, Faculty of Chemistry, Noakowskiego 3, 00-664 Warszawa, Poland

* Corresponding author, e-mail:
michal.mlotek@pw.edu.pl

Abstract

Hydrogen has been identified as an essential component of a decarbonized and sustainable energy system. The use of hydrogen is associated with the problem of its storage and distribution. Storing hydrogen in the gaseous state is energy-consuming, mainly due to the process of its compression. A much higher density of hydrogen can be obtained after its liquefaction. Hydrogen can also bond in chemical compounds, for example, in ammonia which contains 17.8% hydrogen by weight. The aim of the work was to examine the ammonia decomposition process in the plasma-catalytic system and to determine the effect of the process parameters on energy consumption. The applied catalysts allowed higher ammonia conversion than the homogeneous system. The lowest energy consumption, 593 kJ/molH$_2$, was obtained for the 10% Fe/Al$_2$O$_3$ catalyst. The highest ammonia conversion (approx. 90%) was obtained using the 10% Co/Al$_2$O$_3$ catalyst.

Keywords

plasma-catalytic process, ammonia decomposition, gliding discharge, hydrogen

1. INTRODUCTION

The depletion of fossil fuels and their negative impact on the environment led to the search for alternative energy sources, such as H$_2$, which has been identified as an essential component of a decarbonized and sustainable energy system (Chapman et al., 2019; Dawood et al., 2020; Parra et al. 2019). Hydrogen can be obtained from fossil fuels and biomass using conventional thermal processes (steam reforming, gasification, pyrolysis), water electrolysis, or photoelectrolysis using renewable energy sources. Steam methane reforming is the most common and cost-effective method of obtaining hydrogen (Edwards et al., 2007, Uddin et al., 2020). It is a highly endothermic reaction conducted at high temperature and pressure in the presence of a supported nickel catalyst. This process produces a gas containing hydrogen, carbon dioxide, and carbon monoxide. The disadvantage of this process is high CO$_2$ emission (Esily et al., 2022). The share of natural gas, crude oil, and coal in hydrogen production is 48%, 30%, and 18%, respectively. Only 4% of the world's hydrogen production comes from water electrolysis (Uddin et al., 2020).

The use of hydrogen is associated with the problem of its storage and distribution. Storing hydrogen in the gaseous state is energy-consuming, especially due to the process of its compression. A much higher density of hydrogen can be obtained after its liquefaction (Acar and Dincer, 2020; Wan et al. 2021). Methods for storing H$_2$ in carbon materials with a high specific surface area, such as activated carbon, graphite, or carbon nanotubes, are investigated (Niaz et al. 2015; Zhang, 2022). Hydrogen can also bond in chemical compounds, for example, in metal hydrides such as Li, Na, and Mg or in ammonia (Rusman and Dahari, 2016; Schneemann et al., 2018).

Ammonia contains 17.8% hydrogen by weight (Aziz et al., 2020). Ammonia is industrially obtained by the Haber and Bosch process, and its transport or storing methods are well-known and refined. To enable the use of ammonia as a chemical hydrogen storage, it is necessary to develop an efficient method of its decomposition to hydrogen and nitrogen.

Ammonia decomposition is an endothermic process carried out in the presence of a catalyst at high temperatures (Chiuta et al., 2013). In the process of ammonia decomposition, alloys, monometallic, bimetallic, and multimetallic catalysts deposited on oxides or carbon supports are used (Bell and Torrente-Murciano, 2016; Huang et al., 2019; Kalamaras and Efstathiou, 2013; Li et al., 2005; Morlanés et al., 2021; Schüth et al., 2012; Su et al., 2018; Tabassum et al., 2022; Varisli and Kaykac 2016; Wan et al., 2021; Wang et al., 2019; Yin et al., 2004). It should be noted that the catalysts may be deactivated if ammonia is not purified.

Plasma methods of ammonia decomposition can be an alternative method to catalytic processes. Ammonia conversion can be conducted using non-equilibrium plasma generated in electrical discharges. Non-equilibrium plasma can be combined with a catalyst, accelerating chemical reactions (Akiyama et al., 2018; El-Shafie et al., 2020; Fateev et al., 2005; Hayakawa et al., 2020; Lin et al., 2021; Młotek et al., 2021; Qiu et al., 2004; Zhao et al., 2013). The advantage of using a plasma-catalytic system is no need to preheat the gas. The increase in temperature is caused by the supplied electric energy, which is used to generate high-energy electrons (Młotek et al., 2021). Different types of discharges were investigated, such as dielectric barrier discharge, corona discharge, or gliding discharge. In this paper, the decomposition of ammonia in

the gliding discharge was conducted since this type of reactor has a simple design and can be powered by various power supplies. An important advantage of the gliding discharge is the ability to use high flow rates of the gas. Moreover, gliding discharge makes it possible to run the process at atmospheric pressure under constant conditions for an extended time. The aim of the work was to examine the ammonia decomposition process in the plasma-catalytic system and to determine the effect of the process parameters on energy consumption.

The novelty of the study is the use of a plasma-catalytic system with a gliding discharge for ammonia decomposition. The process was conducted using variable discharge power and catalysts: Co/Al_2O_3, and Fe/Al_2O_3. The measurements were carried out for different initial concentrations of ammonia.

2. EXPERIMENTAL SETUP

The gliding discharge reactor was made of a quartz tube with a 40 mm diameter and height of 255 mm. The reactor volume was 0.4 dm^3, and the volume of the zone where the plasma was generated was about 0.2 dm^3 (Fig. 1). The electrodes were placed vertically, and the gap at the point of ignition of the discharge was 3 mm.
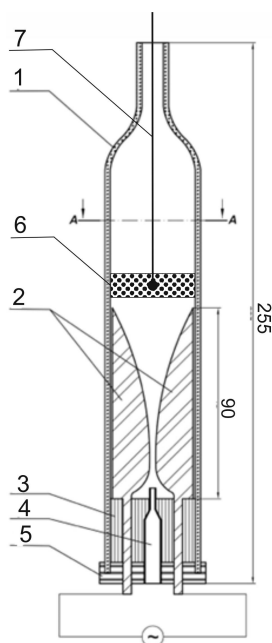

Figure 1. The gliding discharge reactor. 1 – quartz tube, 2 – steel electrodes, 3 – ceramic ring, 4 – gas inlet, 5 – teflon insulation, 6 – catalyst bed, 7 – thermocouple.

The reactor was supplied with alternating current at 50 Hz frequency. The power supply consisted of Fart Resinblock 200 high-voltage transformer and an AEWS E01A thyristor power regulator. The power supply voltage and current limits were 8 kV and 100 mA, respectively. The discharge power was measured with an energymeter Orno OR-WE 512.

The process of ammonia decomposition was conducted using the initial concentration of ammonia (purity of 99.85%) 5–27% mixed with nitrogen (purity of 99.999%). Gas flow rates were regulated by mass flow controllers (MFC1 Bronkhorst Mass-Stream and MFC2 Bronkhorst EL-Flow in Figure 2). After passing through the regulators, the gas streams were connected and mixed before introducing them into the reactor. The catalyst bed (30 cm^3) was 7 mm above the electrodes. (Fig. 1). During the process, the temperature of the catalyst bed was measured using a type K thermocouple.
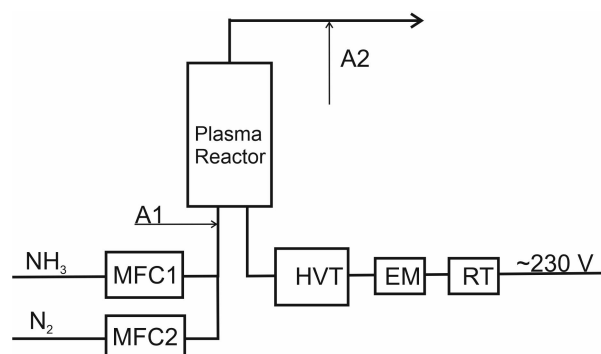

Figure 2. Schematic diagram of apparatus for ammonia decomposition in gliding discharge plasma: MFC1, MFC2 – mass flow controllers, HVT– high voltage transformer, EM – energy meter, RT – thyristor power regulator, A1, and A2 – sampling points.

The ammonia content in the gas introduced to the reactor was determined by the titration weight method. For the gas collecting, the flask containing about 50 ml of water was used. It was under the pressure of about 100 hPa. The flask was weighed and, after that, connected to point A1 or A2 for gas sampling. After the gas was collected, the flask was disconnected and weighed again. The solutions were titrated with 0.1 mol sulphuric acid (VI) with methyl red indicator. Using the titration-weight method, it was possible to calculate the ammonia concentration in the inlet and outlet gas and, based on it, the ammonia conversion during the process. The outlet gas was analyzed with a gas chromatograph (Chrompack CP 9002, equipped with a TCD detector) to determine the hydrogen mole fraction. For each catalyst, the ammonia decomposition was measured at the initial concentrations of 5%, 10%, 18%, and 27%. The discharge power was in the range of 50–300 W. The ammonia decomposition was conducted using a total gas flow rate of 180 l/h.

2.1. Preparation of catalysts

The catalysts, 10% Co/Al_2O_3 and 10% Fe/Al_2O_3, were obtained by dry impregnation with hydrated salts cobalt or ferric nitrate. α-Al_2O_3 with a grain size of 2 mm. The prepared carrier was added quickly to the salt solution and heated till the water evaporated. The catalysts were dried at 120 °C for 24 hours. After that, the catalysts were calcined in an oven at 450 °C for 5 hours.

2.2. Parameters and Definitions

The following definitions were used for the calculations:

Ammonia conversion in plasma catalytic system:

$$X_{\text{NH}_3} = \frac{W_0\,[\text{A}] - W\,[\text{A}]}{W_0[\text{A}]} \tag{1}$$

where, $W_0\,[\text{A}]$ – initial ammonia flow rate, mol/h; $W\,[\text{A}]$ – ammonia flow rate at the outlet of the reactor, mol/h.

Energy consumption, to produce 1 mole of hydrogen from ammonia, kJ/mol H_2:

$$Z = \frac{P \cdot 3.6}{1.5 \cdot W_0[\text{A}] \cdot X_{\text{NH}_3}} \tag{2}$$

where, P – discharge power, W.

3. RESULTS AND DISCUSSION

The effect of the initial concentration of ammonia on its conversion for power of 300 W and 180 l/h flow rate is presented in Figure 3. The ammonia conversion decreases in the plasma-catalytic and homogenous systems with the increase in ammonia concentration. The highest conversion (77%) was obtained for the cobalt catalyst, for an initial ammonia concentration of 5%. Over the entire range of used concentrations, the plasma-catalytic systems achieved higher ammonia conversion than the homogenous one (Fig. 3). In the range of initial ammonia concentrations of 5–18% vol., a higher ammonia conversion was achieved using the cobalt catalyst. When an initial ammonia concentration of 27% was used, the iron catalyst was more active. This may be due to a change in the mechanism of the process.
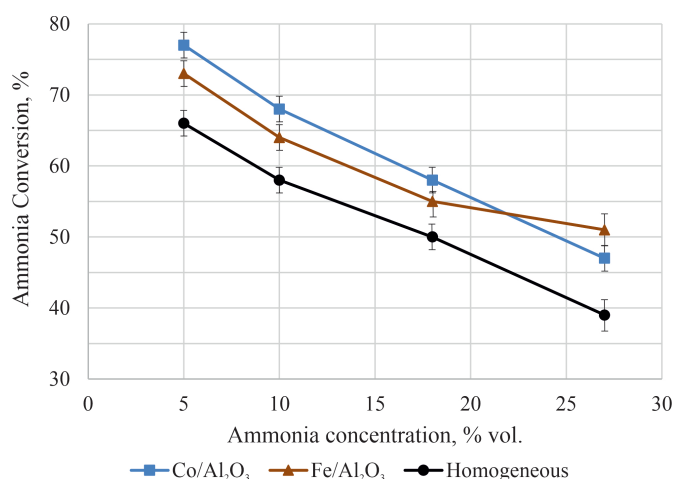

Figure 3. Effect of catalyst on ammonia conversion; discharge power 300 W, gas flow rate 180 l/h.

The influence of the discharge power on the ammonia conversion in its entire range was observed. The conversion increases over the entire range of the initial ammonia concentration

when using the cobalt and iron catalyst. The highest values of $X\,NH_3$ were 0.77 and 0.73, respectively, for cobalt and iron catalysts (Fig. 4). It was obtained at 300 W discharge power and an initial ammonia concentration of 5% vol.
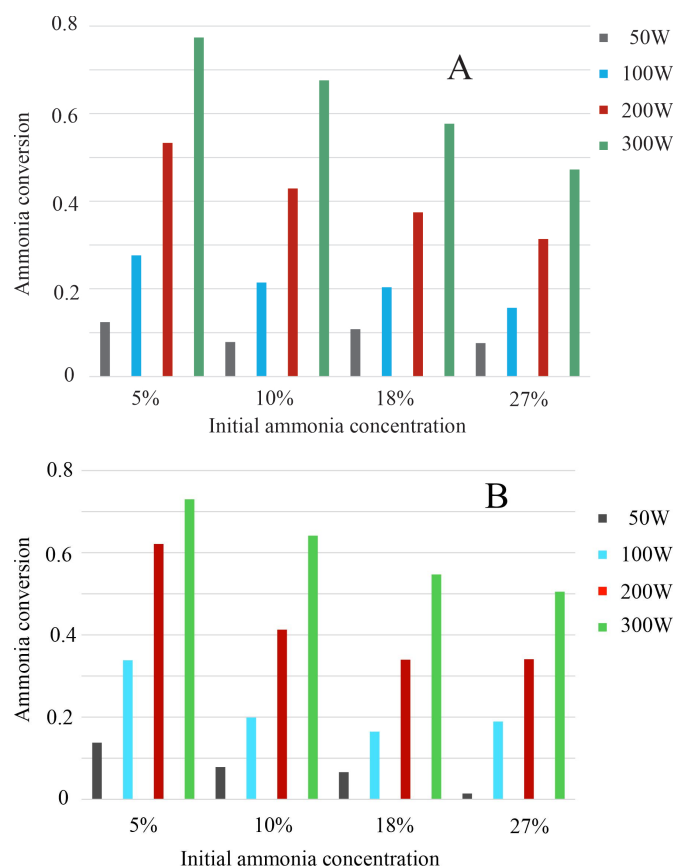

Figure 4. Effect of discharge power on the ammonia conversion in the plasma catalytic system with A – 10% Co/Al_2O_2 and B – 10% Fe/Al_2O_3. Gas flow rate 180 l/h.

In a plasma-catalytic system with Co/Al_2O_3 and 5% NH_3, the energy consumption (Z) in the 50–100 W discharge power range decreases, while an increase in Z was observed for 200–300 W (Table 1). Energy consumption at an initial ammonia concentration of 5 and 10% vol. is significantly higher than at concentrations of 18 and 27% vol. The energy consumption (Z) for NH_3 concentration: 10, 18, and 27 % in plasma-catalytic system changes slightly with the discharge power change, suggesting that the energy consumption slightly depends on the discharge power. The lowest energy consumption occurred for the initial concentration of 27% and the highest for 5% – this value is more than three times higher (Fig. 5, Table 1).

In the plasma-catalytic system with Fe/Al_2O_3 and 5% initial ammonia concentration in the range of discharge power 50–100 W, the energy consumption (Z) decreases. An increase of Z to the value of 2427 kJ/mol H_2 at the discharge power of 300 W was observed. Energy consumption decreases with an increase in discharge power for 10% of ammonia. The lowest Z (593 kJ/molH_2) was observed for an initial concentration
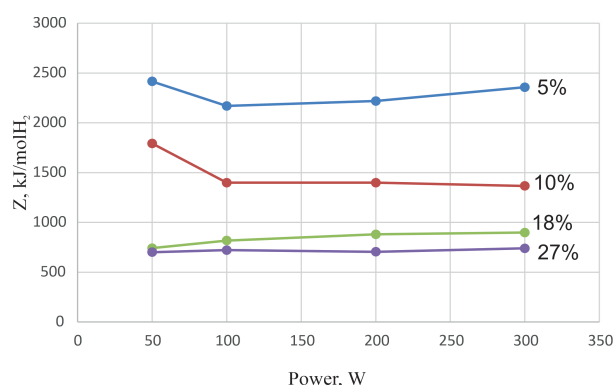
Figure 5. Effect of discharge power on the Energy consumption (Z) in the plasma catalytic system with Co/Al$_2$O$_3$; gas flow rate 180 l/h.

Changes in energy consumption result from the activity of the catalysts in given conditions and are related to the achieved ammonia conversion at the given discharge power. With a low NH$_3$ content in the gas, despite high conversion, a small amount of hydrogen is produced quantitatively. Hence, the energy consumption is high. A large part of the supplied energy is not used for the ammonia decomposition process but, for example, to excite the nitrogen in the gas. Using an initial NH$_3$ concentration of 27%, lower conversion rates are achieved than with 5%, but more moles of hydrogen are produced. When using a higher initial concentration of ammonia, a greater part of the energy supplied to the reaction in gliding discharge is used in the NH$_3$ decomposition process because there is a higher probability of the high-energy electron to collide with the ammonia molecule.

of 27% and a discharge power of 100 W. In this concentration, at 300 W discharge power, the energy consumption was 688 kJ/mol H$_2$ (Table 1). It was 3.5 times less than at 5% ammonia initial concentration. The results obtained for the Fe and Co catalysts were compared with the previous results (Zhang et al., 2022) obtained in the homogeneous system (without the catalyst). The catalyst bed presence influenced the obtained energy consumption (Z). Lower energy consumption Z for the 5% initial ammonia concentration was obtained in the entire range of discharge powers used in the plasma-catalytic system (Table 1).

Both in the plasma-catalytic and homogeneous system, the lowest energy consumption Z was obtained at the highest initial ammonia concentration of 27%. In a plasma-catalytic system with an iron or cobalt catalyst, energy consumption Z depended to a small extent on the discharge power. In the case of using a discharge power of 150 W, the energy consumption Z per mole of hydrogen obtained in the plasma-catalytic systems was lower by more than 200 kJ/mol H$_2$ than in the homogeneous system. When higher discharge power was used, the difference was negligible and amounted to 100–120 kJ/molH$_2$ (Fig. 6).

Table 1. Energy consumption (Z) in the plasma and plasma-catalytic systems.

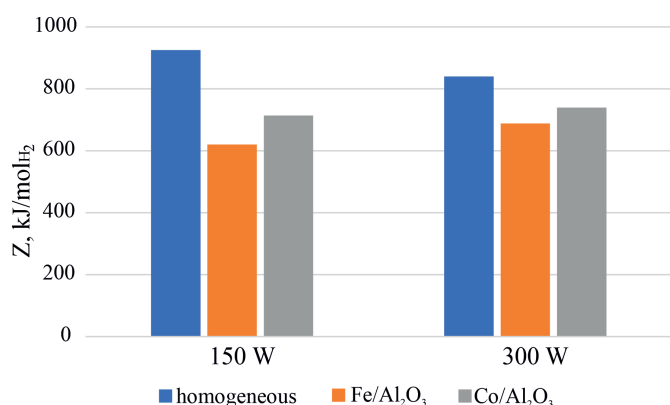| Initial conc. of NH$_3$ [%]	Power [W]	10% Co/Al$_2$O$_3$ Z [kJ/mol H$_2$]	10% Fe/Al$_2$O$_3$ Z [kJ/mol H$_2$]	Without catalyst Z [kJ/mol H$_2$]
5	50	2416	2094	2449
	100	2170	1775	2351
	200	2219	1924	2416
	300	2358	2427	2729
10	50	1793	1944	1336
	100	1399	1478	1336
	200	1399	1440	1336
	300	1367	1436	1644
18	50	742	1163	801
	100	818	973	763
	200	881	963	866
	300	898	935	991
27	50	701	–	900
	100	722	593	1080
	200	705	646	771
	300	740	688	840

Figure 6. Effect of discharge power on the ammonia unit energy consumption at discharge power 150 and 300 W, ammonia initial concentration 27%.

Figure 7. Effect of discharge power and temperature on the ammonia conversion in the plasma-catalytic system with A – 10% Co/Al_2O_3 and B – 10% Fe/Al_2O_3. Gas flow rate 180 l/h, initial ammonia concentration 5%. The digits on the graphs are the temperatures of the catalyst bed in $^{\circ}C$. Red curves – thermally isolated reactor, blue curves – reactor without thermal isolation.

The reactor for the plasma-catalytic system with 10% Co/Al_2O_3 and 10% Fe/Al_2O_3 was thermally isolated and the effect of the increase of catalyst bed temperature on ammonia conversion was investigated. The tests were conducted using an initial ammonia concentration of 5%. It was found that the catalyst temperature influenced the ammonia conversion. The XNH_3 with cobalt catalyst and discharge power up to 200 W did not rise significantly. The ammonia conversion rises to 90% at discharge power 300 W. This might be the effect of the thermal activity of the cobalt catalyst (Fig. 7a). In the case of the iron catalyst, a different conversion profile was obtained. An increase in the process temperature at discharge power up to 270 W caused a significant reduction in the ammonia conversion. Only at the highest applied discharge power of 300 W, an increase of the ammonia conversion to 79% was observed. After reaching the highest temperature of the process, the gliding discharge was turned off and the hydrogen content was measured. Under this condition, negligible amounts of hydrogen were observed, which are most likely residues from the plasma-catalytic process. This indicates that the ammonia decomposition process did not occur without plasma in the examined condition.

Regarding the results obtained with cobalt and iron catalysts, one can conclude that for the cobalt catalyst, no influence of temperature on the nature of the curves was observed. The increase of the temperature of the iron catalyst at the respective discharge power resulted in a decrease of ammonia conversion and a change in the nature of the curve (Fig. 7). This may result from the reaction of the NH_2 radical with the H_2 formed during the process, resulting in the regeneration of the ammonia molecule.

The influence of the initial concentration of ammonia on its decomposition was found. When using low concentrations of NH_3 (5–27%) in nitrogen, the presence of N_2 is beneficial and increases the ammonia conversion. This might be a result of a higher concentration of nitrogen in excited states, which leads to the number of active collisions with ammonia molecules, resulting in ammonia dissociation (Młotek et al.,
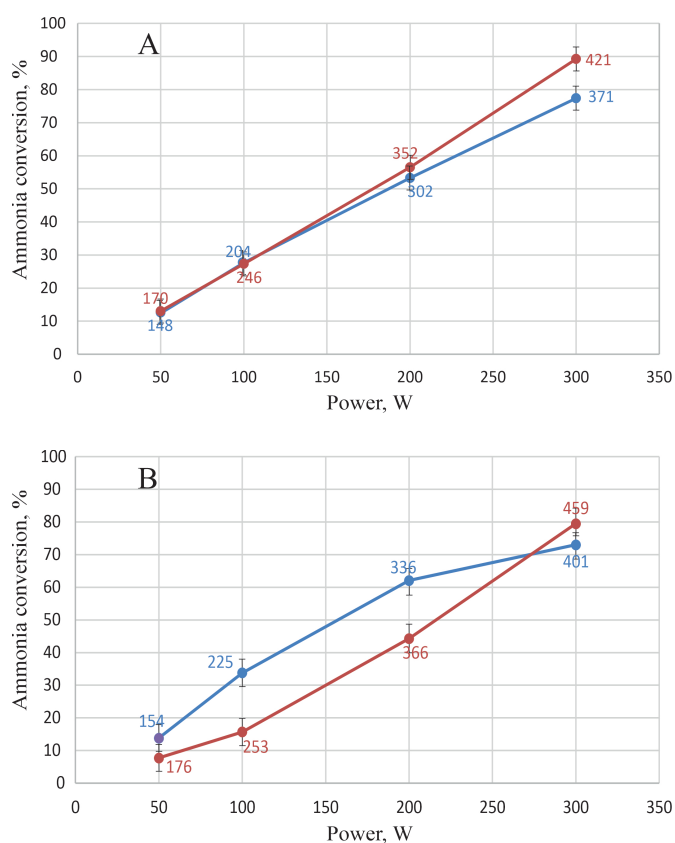
2021). However, energy consumption rises with an increase in nitrogen concentration. Plasma-catalytic ammonia decomposition was initiated by a collision of ammonia molecules with excited nitrogen or high-energy electrons. The detailed mechanism of plasma decomposition of ammonia was described in our previous article (Ertl, 1991; Młotek et al., 2021). In the plasma process, NH_2, NH, H, and NNH radicals can be formed. The reactions of NNH radicals are very fast, so they cannot reach the catalyst surface, but nitrogen and hydrogen can be formed (reactions R1–R3).

$$NNH + H \rightarrow N_2 + H_2 \qquad (R1)$$

$$NNH + N \rightarrow NH + N_2 \qquad (R3)$$

$$NNH + NH \rightarrow N_2 + NH_2 \qquad (R3)$$
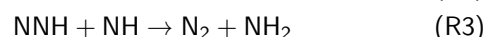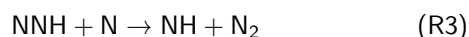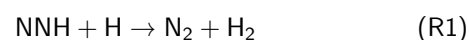
Radicals NH_2, NH, H, or excited nitrogen are more stable and can reach the catalyst surface and adsorb. On the catalyst surface, two kinds of processes may occur: further decomposition into N_2 and H_2

$$NH_2 \leftrightarrows NH + H \qquad (R4)$$

$$NH + N \rightarrow N_2 + H \qquad (R5)$$
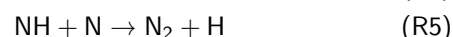
or recombination of NH_2 or NH radicals with hydrogen radicals to regenerate ammonia

$$NH + H \rightarrow NH_2 \tag{R6}$$
$$NH_2 + H \rightarrow NH_3 \tag{R7}$$

4. CONCLUSIONS

The results prove the possibility of using a plasma-catalytic system of a gliding discharge plasma to conduct the ammonia decomposition process. The applied catalysts allowed higher ammonia conversion than the homogeneous system. The initial ammonia concentration and the discharge power had a significant impact on the value of the ammonia conversion and the energy consumption required to obtain a mole of hydrogen. The highest ammonia conversion (approx. 90%) was obtained using the 10% Co/Al_2O_3 catalyst at the temperature of 421 ºC obtained with thermal isolation of the catalytic part of the reactor. The temperature affects the plasma-catalytic conversion of ammonia. An increase in temperature increases the ammonia conversion in the case of a 10% Co/Al_2O_3 catalyst. In the plasma-catalytic system with an iron catalyst, at temperatures above 200 °C, recombination of H and NH_2 radicals may form ammonia, increasing the energy consumption to obtain a mole of H_2.

ACKNOWLEDGMENTS

REFERENCES

Acar C., Dincer I., 2020. The potential role of hydrogen as a sustainable transportation fuel to combat global warming. *Int. J. Hydrogen Energy*, 45, 3396–3406. DOI: 10.1016/j.ijhydene.2018.10.149.

Akiyama M., Aihara K., Sawaguchi T., Matsukata M., Iwamoto M., 2018. Ammonia decomposition to clean hydrogen using non-thermal atmospheric-pressure plasma. *Int. J. Hydrogen Energy*, 43, 14493–14497. DOI: 10.1016/j.ijhydene.2018.06.022.

Aziz M., Wijayanta A.T., Nandiyanto A.B.D., 2020. Ammonia as effective hydrogen storage: a review on production, storage and utilization. *Energies*, 13, 3062. DOI: 10.3390/en13123062.

Bell T.E., Torrente-Murciano L., 2016. H2 Production via ammonia decomposition using non-noble metal catalysts: a review. *Top. Catal.,* 59, 15–16. DOI: 10.17863/CAM.835.

Chapman A., Itaoka K., Hirose K., Davidson F.T., Nagasawa K., Lloyd A.C., Webber M.E., Kurban Z., Managi S., Tamaki T., Lewis M.C., Hebner R.E., Fujii Y., 2019. A review of four case studies assessing the potential for hydrogen penetration of the future energy system. *Int. J. Hydrogen Energy*, 44, 6371–6382. DOI: 10.1016/j.ijhydene.2019.01.168.

Chiuta S., Everson R.C., Neomagus H.W.J.P., van der Gryp P., Bessarabov D.G., 2013. Reactor technology options for distributed hydrogen generation via ammonia decomposition: a review. *Int. J. Hydrogen Energy,* 38, 14968–14991. DOI: 10.1016/j.ijhydene.2013.09.067.

Dawood F., Anda M., Shafiullah G.M., 2020. Hydrogen production for energy: an overview. *Int. J. Hydrogen Energy*, 45, 3847–3869. DOI: 10.1016/j.ijhydene.2019.12.059.

Edwards P.P., Kuznetsov V.L., David W.I.F., 2007. Hydrogen energy. *Philos. Trans. R. Soc. A*, 365, 1043–1056. DOI: 10.1098/rsta.2006.1965.

El-Shafie M., Kambara S., Hayakawa Y., 2020. Alumina particle size effect on H_2 production from ammonia decomposition by DBD plasma. *Energy Rep.*, 6, 25–30. DOI: 10.1016/j.egyr.2020.10.032.

Esily R.R., Chi Y., Ibrahiem D.M., Chen Y., 2022. Hydrogen strategy in decarbonization era: Egypt as a case study. *Int. J. Hydrogen Energy*, 47, 18629–18647. DOI: 10.1016/j.ijhydene.2022.04.012.

Fateev A., Leipold F., Kusano Y., Stenum B., Tsakadze E., Bindslev H., 2005. Plasma chemistry in an atmospheric pressure Ar/NH_3 dielectric barrier discharge. *Plasma Process. Polym.*, 2, 193–200. DOI: 10.1002/ppap.200400051.

Hayakawa Y., Kambara S., Miura T., 2020. Hydrogen production from ammonia by the plasma membrane reactor. *Int. J. Hydrogen Energy*, 45, 32082–32088. DOI: 10.1016/j.ijhydene.2020.08.178.

Huang C., Yu Y., Yang J., Yan Y., Wang D., Hu F., Wang X., Zhang R., Feng G., 2019. Ru/La_2O_3 catalyst for ammonia decomposition to hydrogen. *Appl. Surf. Sci.*, 476, 928–936. DOI: 10.1016/j.apsusc.2019.01.112.

Ertl R., 1991. Elementary steps in ammonia synthesis, In: Jennings J.R. (Ed.), *Catalytic ammonia synthesis. Fundamentals and practice.* Springer, Boston, MA, 109–132. DOI: 10.1007/978-1-4757-9592-9_3.

Kalamaras C.M., Efstathiou A.M., 2013. Hydrogen production technologies: Current state and future developments. *Conference Papers in Science*, 690627. DOI: 10.1155/2013/690627.

Li X.-K., Ji W.-J., Zhao J., Wang S.-J., Au C.-T., 2005. Ammonia decomposition over Ru and Ni catalysts supported on fumed SiO_2, MCM-41, and SBA-15. *J. Catal.*, 236, 181–189. DOI: 10.1016/j.jcat.2005.09.030.

Lin Q.F., Jiang Y.M., Liu C.Z., Chen L.W., Zhang W.J., Ding J., Li J.G., 2021. Instantaneous hydrogen production from ammonia by non-thermal arc plasma combining with catalyst. *Energy Rep.*, 7, 4064–4070. DOI: 10.1016/j.egyr.2021.06.087.

Młotek M., Perron M., Krawczyk K., 2021. Ammonia decomposition in a gliding discharge plasma. *Energy Technol.*, 9, 2100677. DOI: 10.1002/ente.202100677.

Morlanés N., Katikaneni S.P., Paglieri S.N., Harale A., Solami B., Sarathy S.M., Gascon J., 2021. A technological roadmap to the ammonia energy economy: Current state and missing technologies. *Chem. Eng. J.*, 408, 127310. DOI: 10.1016/j.cej.2020.127310.

Niaz S., Manzoor T., Pandith A.H., 2015. Hydrogen storage: materials, methods, and pperspectives. *Renewable Sustainable Energy Rev.*, 50, 457–469. DOI: 10.1016/j.rser.2015.05.011.

Parra D., Valverde L., Pino F.J., Patel M.K., 2019. A review on the role, cost and value of hydrogen energy systems for deep decarbonization. *Renewable Sustainable Energy Rev.,* 101, 279–294. DOI: 10.1016/j.rser.2018.11.010.

Qiu H., Martus K., Lee W.Y., Becker K., 2004. Hydrogen generation in a microhollow cathode discharge in high-pressure ammonia-argon gas mixtures. *Int. J. Mass Spectrom.,* 233, 19–24. DOI: 10.1016/j.ijms.2003.08.017.

Rusman N.A.A., Dahari M., 2016. A review on the current progress of metal hydride material for solid-state hydrogen storage applications. *Int. J. Hydrogen Energy*, 41, 12108–12126. DOI: 10.1016/j.ijhydene.2016.05.244.

Schneemann A., White J.L., Kang S., Jeong S., Wan L.F., Cho E.S., Heo T.W., Prendergast D., Urban J.J., Wood B.C., Allendorf M.D., Stavila V., 2018. Nanostructured Metal Hydrides for Hydrogen Storage. *Chem. Rev.*, 118, 10775–10839. DOI: 10.1021/acs.chemrev.8b00313.

Schüth F., Palkovits R., Schlögl R., Su D.S., 2012. Ammonia as a possible element in energy infrastructure: catalysts for ammonia decomposition. *Energy Environ. Sci.*, 5, 6278–6289. DOI: 10.1039/c2ee02865d.

Su Q., Gu L.L., Zhong A.H., Yao Y., Ji W.J., Ding W.P., Au C.T., 2018. Layered double hydroxide derived Mg_2Al-LDO supported and K-modified Ru catalyst for hydrogen production via ammonia decomposition. *Catal. Lett.*, 148, 894–903. DOI: 10.1007/s10562-017-2195-1.

Tabassum H., Mukherjee S., Chen J., Holiharimanana D., Karakalos S., Yang X., Hwang S., Zhang T., Lu B., Chen M., Tang Z., Kyriakidou E.A., Ge Q., Wu G., 2022. Hydrogen generation via ammonia decomposition on highly efficient and stable Ru – free catalysts: approaching complete conversion at 450 °C. *Energy Environ. Sci.*, 15, 4190–4200. DOI: 10.1039/D1EE03730G.

Uddin M.N., Nageshkar V.V., Asmatulu R., 2020. Improving water-splitting efficiency of water electrolysis process via highly conductive nanomaterials at lower voltages. *Energy Ecol. Environ.*, 5, 108–117. DOI: 10.1007/s40974-020-00147-5.

Varisli D., Kaykac N.G., 2016. Hydrogen from ammonia over cobalt incorporated silicate structured catalysts prepared using different cobalt salts. *Int. J. Hydrogen Energy*, 41, 5955–5968. DOI: 10.1016/j.ijhydene.2016.02.097.

Wan Z., Tao Y., Shao J., Zhang Y., You H., 2021. Ammonia as an effective hydrogen Carrier and a clean fuel for solid oxide fuel cells. *Energy Convers. Manage.*, 228, 113729. DOI: 10.1016/j.enconman.2020.113729.

Wang Z., Qu Y., Shen X., Cai Z., 2019. Ruthenium catalyst supported on Ba modified ZrO_2 for ammonia decomposition to CO_x-free hydrogen. *Int. J. Hydrogen Energy*, 44, 7300–7307. DOI: 10.1016/j.ijhydene.2019.01.235.

Yin S.F., Xu B.Q., Zhou X.P., Au C.T., 2004. A mini-review on ammonia decomposition catalysts for on-site generation of hydrogen for fuel cell applications. *Appl. Catal., A: Gen.*, 277, 1–9. DOI: 10.1016/J.APCATA.2004.09.020.

Zhang H., Zhu Y., Liu Q., Li X., 2022. Preparation of porous carbon materials from biomass pyrolysis vapors for hydrogen storage. *Appl. Energy*, 306, 118131. DOI: 10.1016/j.apenergy.2021.118131.

Zhao Y., Wang L., Zhang J., Gong W., Guo H., 2013. Decomposition of ammonia by atmospheric pressure AC discharge: catalytic effect of the electrodes. *Catal. Today*, 211, 72–77. DOI: 10.1016/j.cattod.2013.03.027.